INTERNATIONAL JOURNAL OF AUTOMOTIVE AND MECHANICAL ENGINEERING
ISSN: 2229-8649 e-ISSN: 2180-1606
VOLUME 22, ISSUE 4, 2025, 12887 - 12902
DOI: https://doi.org/10.15282/ijame.22.4.2025.4.0981

RESEARCH ARTICLE

Impact of Outlet Vent Configurations on Indoor Environmental Quality, Occupant Comfort, and Energy Efficiency: An Optimisation Study

Ghogare Abhijeet Ganesh[1]*, Shobha Lata Sinha[2], Vijay Panchore[3], Tikendra Nath Verma[3]

[1]MAEER's Maharashtra Institute of Technology, Mumbai, Bharat, Maharashtra, 401107, India
[2]Department of Mechanical Engineering, National Institute of Technology Raipur, 492013, India
[3]Department of Mechanical Engineering, Maulana Azad National Institute of Technology, Bhopal, 462003, India

ABSTRACT – The rising demand for building energy and the time spent indoors are driving the need for a sustainable balance between building energy demand and occupant comfort. The detailed analysis of fluid flow, radiation heat transfer, heat load on a radiator, and the comfort of indoor occupants is essential for sustainable buildings. This study numerically evaluates the well-validated 3D empty-room model for energy demand in a cold-climate environment to support occupant comfort. Efforts have been made to optimise the factors affecting occupant comfort and the energy demand of the office room to maintain sustainable stability. A well-validated 3-dimensional model simulated airflow, heat transfer, and occupant comfort. The study optimises factors affecting comfort and energy use using multi-objective optimisation (MOO) techniques. Outlet vent location significantly impacts indoor comfort, energy, and fluid flow. Indoor environments can be optimised for both energy and comfort, especially in symmetrical indoor spaces. Floor-level vents improve air circulation but have little impact on energy use in cold climates. In symmetrical fluid domains, symmetrical outlet vent placement achieved the lowest objective function value (0.026), with a heat load of 412.27 W, PMV of 0.24, and PPD of 7.12, whereas floor-level outlet vents showed the highest objective function value (0.575), with PMV of 0.51 and PPD of 12.11, indicating reduced comfort. Overall, optimising ventilation strategies allows for prioritising occupant comfort and energy efficiency based on specific needs.

ARTICLE HISTORY
Received : 16th Oct. 2024
Revised : 07th July 2025
Accepted : 29th July 2025
Published : 15th Nov. 2025

KEYWORDS
PMV
PPD
Energy efficiency
Optimisation
Thermal comfort

1. INTRODUCTION

There is an exponential increase in building energy demand driven by rapid urbanisation and controlled indoor environments [1]. Research shows that 90% of urban residents' lives are spent within enclosed indoor environments [2]. Individuals spend a significant amount of time indoors; therefore, ensuring indoor comfort is vital to the health of indoor occupants. As the duration of indoor time increases, the energy required to maintain indoor comfort also rises. Indoor occupants account for 70% of the total worldwide energy demand to maintain acceptable Indoor Environmental Quality (IEQ) in various types of occupied residential and industrial structures. It is crucial to strike a balance between IEQ standards and energy demand to address the increasing global energy consumption [3]. The global energy crisis that affected cold-climate regions in 2022 highlighted the need to analyse IEQ and develop efficient building plans that prioritise optimal indoor comfort. IEQ includes a broad range of physiological and psychological factors. Key physiological characteristics that affect the indoor environment include indoor air temperature, air movement, occupant activity level, occupant clothing insulation, and indoor air quality (IAQ) [4]. In recent energy-intensive mechanical ventilation and heating systems, energy is the primary means of attaining IEQ and IAQ. There is a considerable risk of widespread system failure due to the growing energy demand, which accounts for 55–65% of worldwide energy use [5]. It is imperative to manage IEQ sustainably to meet the rising energy demands required to maintain building comfort. Natural ventilation (NV) stands out as a viable alternative for reducing building energy consumption. It can significantly reduce the energy required to maintain acceptable IEQ and IAQ by utilising natural convection to transport heat within a precisely regulated indoor environment. The implementation of NV methods has emerged as a crucial component of sustainable building development. This method leverages the advantages of buoyant forces by exploiting differences in air pressure and density [6]. The Heating, Ventilation, and Air Conditioning (HVAC) efficacy of NV structures depends on various factors, including the building envelope design, external environmental conditions, window configurations, air inlet and outlet vent positions or locations. Diverse approaches to optimising the potential of NV buildings through envelope design are necessary. NV systems offer an acceptable IEQ suited for both hot and cold climates, drawing attention to energy efficiency and the advancement of sustainable building practices [6].

The location of the inlet and exhaust ventilation is crucial to maintain adequate IEQ and diffuse inlet fresh air when designing an efficient building envelope. The position of the inlet and outlet vents has a significant impact on the installation of the cooling and heating device [7]. The proper location of the exhaust and inlet influences indoor energy demand and indoor pollution control, as well as acceptable IEQ. Vent positions similarly influence thermal stratification layers, which, in turn, affect comfort and energy demand [8]. Another study found that up to 20.8% of energy savings

*CORRESPONDING AUTHOR | G.A. Ganesh | ✉ abhigg3@gmail.com

resulted from positioning the inlet at ground level and exhaust ventilation adjacent to the inhabited space [9]. In cold regions, the air inlet for an NV space should be positioned near the heating panel to ensure a sufficient mixture of hot and cold streams. The careful positioning of radiators maximises the indoor well-being of occupants and reduces building energy demands. It allows for the expansion of an occupied zone and the reduction of the mixing zone. In cold climate conditions, placing the inlet vent above the radiator panel significantly improves energy efficiency and indoor comfort, while the exhaust vent position affects contamination control in hospital facilities [10]. The experimental and numerical results of the study demonstrate how altering the air exit can impact energy demand and indoor comfort. Cheng et al. found significant energy savings linked to the standard exhaust vent placement by combining the exhaust side and the ceiling-mounted light bulb in their investigation [11]. Variations in the diffuser inlet angle have a similar impact on both comfort and energy demand for maintaining indoor occupant comfort. [12]. An inlet vent perimetric ratio of 4 enhances ventilation effectiveness and reduces indoor contamination. The symmetrical inlet vent placements along the side wall are more effective than asymmetrical sites [13]. The higher input velocities with less efficient aspect ratios lead to higher concentrations of indoor carbon dioxide, underscoring the necessity to develop an ideal ventilation inlet aspect ratio to optimise indoor air quality. The use of a vortex flow device improves IAQ in large structures with intense pollutants [14]. This device quickly and effectively prevents pollutant diffusion using column vortex principles. Numerical investigations have demonstrated its superiority over alternative air supply methods in terms of overall ventilation efficacy and pollutant removal. These ventilation settings can effectively address IAQ issues with this device. The study by Chen et al. [15] investigated particle dispersion for a range of ventilation modes, inlet velocities, and floor temperatures. It demonstrated that the airflow velocity increased with higher floor temperatures due to natural convection. There was a higher concentration of particles in the centre of the chamber, and higher inlet velocity and floor temperature accelerated the removal of particles for upward supply ventilation.

The investigations above have primarily focused on determining the optimal location for building ventilation. Further research is necessary to determine how the exhaust vent specifically affects comfort measures and energy demand. This study examines the impact of exhaust ventilation locations on indoor occupant comfort and energy use by investigating different arrangements of rectangular-shaped outlet vents placed on various walls and at alternative locations. It also determines fluid flow parameters during fresh air inlet and stale air outflow for the different ventilation profiles. The study evaluates the effects of these different ventilation arrangement changes on air temperature, indoor fluid flow, and velocity distribution, which affects the radiator heating load and occupant comfort. Inlet and outlet vent surface areas are kept constant across all sites to ensure a necessary comparison. Assessment of thermal comfort and energy consumption depends on various factors, including but not limited to operating temperature, air velocity, temperature gradient, radiation, and indoor convection [16]. The problem was numerically analysed using the commercial ANSYS simulation software, and the results were further post-processed. Several studies have examined building IEQ, thermal comfort, and energy efficiency, but few have examined how outlet vent configurations affect these parameters. Most studies focus on thermal comfort [17], airflow distribution [18], or energy performance [19] without considering how vent design affects occupant comfort and building energy demand.

CFD-based simulation and multiobjective optimisation have received less attention in optimising vent location, size, and arrangement. This gap is significant in naturally and mixed-ventilated systems, where the outlet location may affect airflow and indoor heat removal [20] [21]. The study aimed to achieve an optimal balance between indoor thermal comfort and energy demand in building design. A multiobjective optimisation approach is applied to maximise occupant comfort while minimising the building energy consumption. The Weighted Sum Method (WSM) was used as the primary optimisation technique to find this balance between indoor comfort and building energy demand. The study ensures the acceptable indoor comfort standards are maintained while reducing energy usage, thereby contributing to more sustainable building design practices that integrate both comfort and energy efficiency.

1.1 Physical Problem

The naturally ventilated numerical simulation was analysed to study the outcomes of altered outlet ventilation sites. The different modelled ventilation settings were designed using the ICEM CFD software. This study conducted numerical analysis with higher precision using computational software, incorporating all relevant modelling aspects. The comprehensive validation of the model was conducted using both numerical and experimental studies on a similar geometric model.

1.1.1 Model description and monitoring lines

The modelling software generated a naturally ventilated room in the ICEM CFD model, with a volume of 31,104 m^3 and dimensions of 4.8 × 2.7 × 2.4 m^3. ANSYS Fluent was used to perform the numerical analysis. This simulated geometric model represents the airflow arrangement in the room, similar to cross ventilation. This office building features six adiabatic walls, including the floor and ceiling, to facilitate a targeted investigation into indoor comfort and energy consumption. The adiabatic conditions were maintained to isolate the indoor fluid domain from the ambient environment and prevent infiltration losses. As shown in Figure 1, adiabatic walls include a roof, input vent wall, exhaust vent wall, and two additional walls (floor and ceiling). A double-panel radiator installation in the modelled design is to heat the cold air entering the room. The details of the geometric model are shown in Table 1.

Table 1. Geometric specifications

Geometry (objects)	(L × B × H)	Position
Walls	4.8 m × 2.7 m	
Walls with an inlet and outlet	2.4 m× 2.7 m	
Ceiling and floor	4.8 m× 2.4 m	
Window	2.4 m× 1.2 m	0.8 m above floor level
Inlet ventilation	0.50 m× 0.02 m	Above window
Outlet ventilation	0.80 m× 0.05 m	A wall opposite the inlet vent
Radiator		Mid-position along the wall and under the window, 0.01 Away from the wall.
Plate 1	1.40 m× 0.05 m× 0.60 m	
Plate 2	1.40 m× 0.05 m× 0.60 m	

Monitoring lines and planes were modelled to analyse IEQ at various locations in the occupied zone. These monitoring lines and planes are essential for assessing comfort-related factors, including air temperature, velocity, temperature gradient, total temperature, and velocity vector contour. A two-dimensional plane is modelled on the XY plane at Z = 0 to measure comfort in the occupied zone. Additionally, monitoring lines (l_1, l_2, l_3, and l_4) were placed at distances of 0.6, 1.8, 3.0, and 4.2 m from the window model to measure the operative temperature. It serves as a key indicator of the overall thermal comfort of the room. The neck and ankle of a seated occupant are generally exposed to indoor air, which creates the sensation of cold air, leading to a cold draft problem. The cold air tends to collect at floor level due to buoyancy near the exposed occupant's ankle area. The horizontal set of monitoring lines drawn at specific points, in addition to the vertical monitoring lines, also plays an important role. It analyses the seated occupant's ankle and neck responses to comfort, as shown in Figure 1(c).

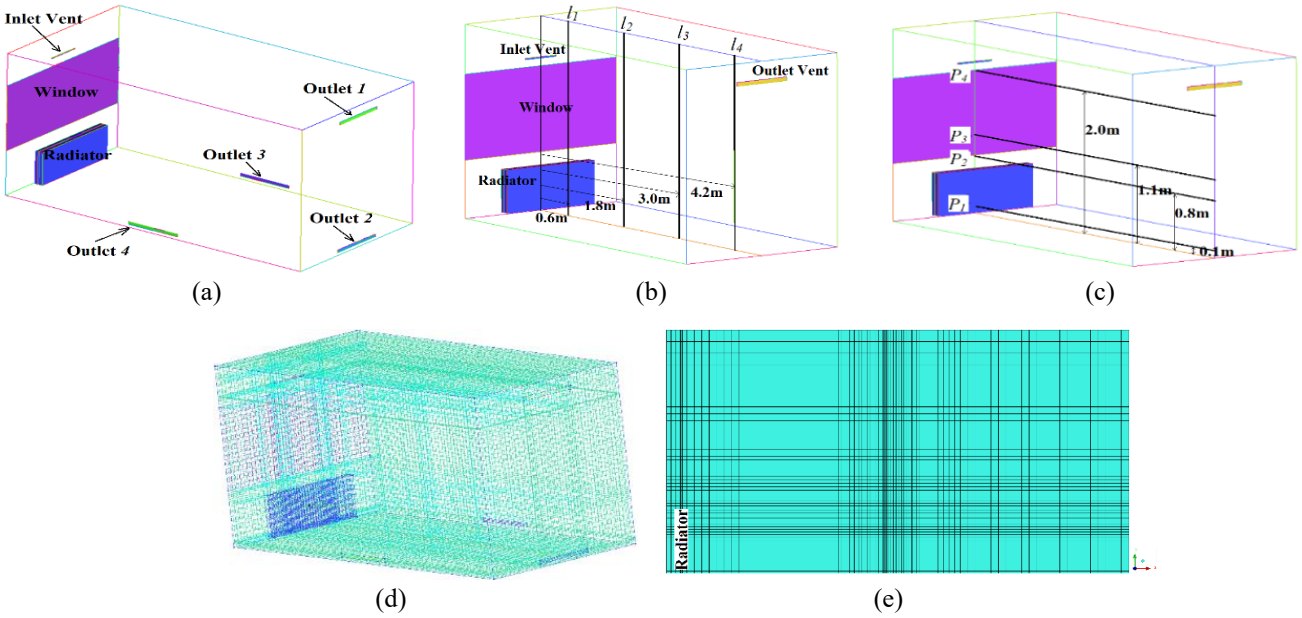

Figure 1. Representation view of 3-D arrangement with hex-mesh (a) empty room model, (b) straight-up monitoring lines, (c) horizontal monitoring lines, (d) hexagonal unstructured mesh, (e) monitoring plane passing through the middle of the room (z = 0)

1.1.2 Boundary conditions

The focus of the research is on IEQ in the typical winter environment in India. In winter, the minimum temperatures can drop as low as 5°C. The pressure difference in a naturally ventilated office building causes outside cold air to enter the structure. The window surface temperature was maintained at 14°C as per the previously done conduction analysis [22]. Radiator and inlet ventilation, located next to the glazed glass window, prevent the indoor air temperature from fluctuating when the outside air temperature falls below 5°C. Due to the significant mixing of cold and hot air streams in this region, the temperature of the indoor air close to the window was approximately 14°C. Myhren et al. [22] comprehensively studied the transfer of heat from indoor to outdoor air through the glass window. Since no artificial fans are used to provide fresh air, ventilation relies on natural convection. According to comfort standards, office buildings should have at least 2.5 l/s/person of ventilation, following ASHRAE norms [2]. For two occupants, a fresh air flow of 5 *l/s* would be the least requirement. An advanced ventilation rate of 8.5 *l/s* was used to ensure the safety of the two individuals as per the activity level. The vent area and inlet air density were kept constant, while the fresh air entering velocity was set to 0.7 m/s as per the standard requirements of constant mass flow rate. The material for the radiator is aluminium, and as the walls are assumed to be adiabatic, their material does not influence the numerical study.

Table 1. Limiting conditions and model specifications

Parameter	Input conditions
Fresh air inlet (For all case studies)	V_{air} = 0.70 m/s $T_{inlet\ air}$ = 5°C
Indoor air exit	Outflow
Glaze the glass window.	T_{window} = 14°C (Constant)
Radiator	Constant heat flux, $T_{Surface}$= 30-32 °C
Walls	Adiabatic Enhanced wall treatment [23]
Computational models	
Turbulent	Standard k-ε [24][25]
Radiation	DO Radiation [26][27]
Scheme for pressure	The second order, a SIMPLE algorithm [28]

Convergence criteria		
Criterion	Description	Value/setting
Residual tolerance	Maximum allowable residual value for convergence in mass, momentum, and energy equations	10-6 (for mass, momentum, energy)
Convergence tolerance for variables	Tolerance for the convergence of key variables such as temperature and velocity	0.1% change between iterations
Physical convergence	Evaluation of stability and change in results between different runs	No significant change between runs
Monitoring parameters	Key parameters monitored for convergence, such as temperature, pressure drop, and velocity	Temperature, velocity, and pressure drop

2. NUMERICAL METHODOLOGY

As mentioned in the introduction section, the goal of this analysis is to study the influence of altered outlet vent locations on the building energy demand and IEQ. This problem solves the continuity, momentum, and energy equations through numerical methods while the inlet–outlet vent area remains unchanged.

2.1 Case Description

Different ventilation settings were analysed to examine the impact of altered outflow vent settings on IEQ, occupant comfort, and building energy demand. The different positions of the outflow and the combination of outlets have been utilised for various cases in the analysis. Table 2 shows the different cases formulated for numerical analyses. The inlet vent location and area were kept similar, while the outlet location varied within the profile, remaining constant across all cases. A total of four different outlet vents have been used in combination. After performing the numerical simulations, analyses of temperature, velocity, and temperature gradient identified the influence of outlet vent location on occupant comfort and energy demand. The governing mass, momentum, continuity, and energy equations were resolved using CFD.

Table 2. Ventilation settings

Ventilation Cases	Inlet	Outlet
1	Above window	Outlet 1
2	Above window	Outlet 2
3	Above window	Outlet 3, Outlet 4
4	Above window	Outlet 2, Outlet 4
5	Above window	All Outlets

2.2 Grid Independence Test

The geometric model has been discretised using a hexagonal mesh to ensure optimal mesh control, with further refinement applied to the fluid domain requiring higher precision. An essential mesh independence test was performed to ensure the model's independence on mesh size. This test assesses the impact of grid size variations on the simulation results. The results should exhibit minimal sensitivity to mesh size, confirming solution accuracy and resource efficiency for the ideal computational model. Three different mesh configurations were studied for this analysis, comprising 179,000, 289,000, and 386,000 nodes, respectively, to conduct a comprehensive mesh independence test on the empty room model.

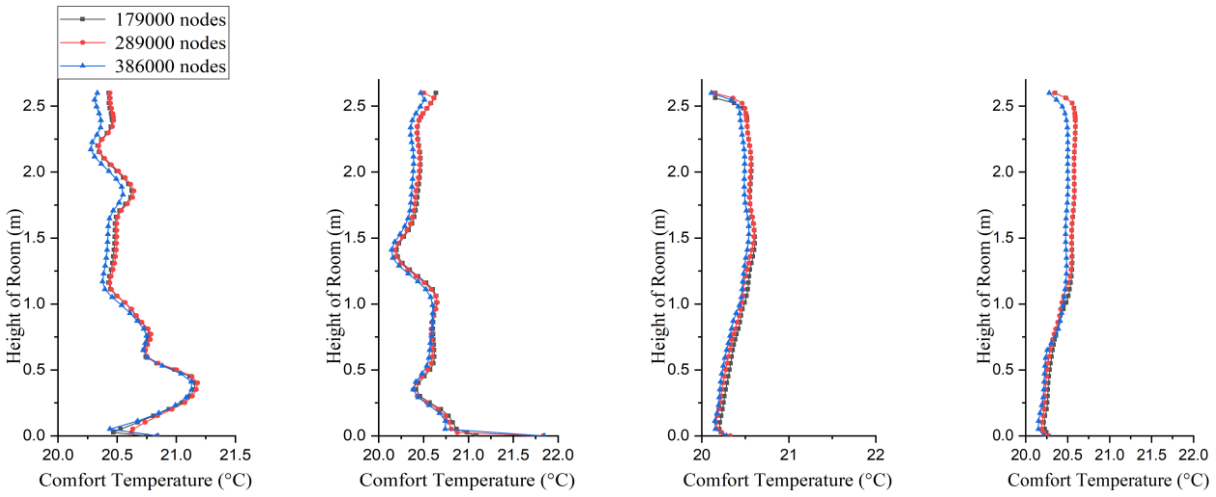

Figure 2. Grid independence test (a) h_1=0.6m, (b) h_2=1.8m, (c) h_3=3.0m, (d) h_4 =4.2m

Figure 2 illustrates the comfort temperature trends observed for the same geometry discretised with three different mesh resolutions. The results show negligible influence of mesh size variation, with deviations in comfort temperature remaining within ±0.07 °C. The study selected the geometric model with the coarse mesh (179,000 nodes) for future studies to optimise computational time and cost. However, for scenarios requiring enhanced accuracy, particularly in the occupied zone or near occupants, localised mesh refinement can be employed. A model with 289,000 nodes was selected for further simulations by balancing accuracy and computational cost based on this analysis. The comfort temperature results were calculated using the root mean square error (RMSE) for Figure 2. Figure 2 (a) has an RMSE of 0.2°C, (b) 0.32°C, (c) 0.27°C, and (d) 0.24°C. The average comfort temperature RMSE is 0.25°C. Comparing the ITC results from Olesen et al. and Horikiri et al. yields a maximum deviation of ±0.7 °C and an RMSE of 0.25°C, indicating that they are acceptable for further analysis.

2.3 Numerical Model

In numerical analysis, it is required to solve the mass, momentum, and energy equations to numerically examine a specific fluid domain problem (Equations 1-5). Discrete-Ordinate radiation model and the conventional k-ε turbulent model, which account for internal radiation and turbulence effects, respectively, were used in the CFD program to solve equations 6, 7, and 8 [29]-[31].

$$\frac{\partial \rho}{\partial t} + \nabla.(\rho \vec{V}) = 0 \tag{1}$$

$$\frac{\partial(\rho u)}{\partial t} + \nabla.(\rho u \vec{V}) = -\frac{\partial p}{\partial x} + \frac{\partial \tau_{xx}}{\partial x} + \frac{\partial \tau_{yz}}{\partial y} + \frac{\partial \tau_{zx}}{\partial z} + \rho f_x \tag{2}$$

$$\frac{\partial(\rho u)}{\partial t} + \nabla.(\rho v \vec{V}) = -\frac{\partial p}{\partial y} + \frac{\partial \tau_{xy}}{\partial x} + \frac{\partial \tau_{yy}}{\partial y} + \frac{\partial \tau_{yz}}{\partial z} + \rho f_y \tag{3}$$

$$\frac{\partial(\rho w)}{\partial t} + \nabla.(\rho w \vec{V}) = -\frac{\partial p}{\partial z} + \frac{\partial \tau_{xz}}{\partial x} + \frac{\partial \tau_{yz}}{\partial y} + \frac{\partial \tau_{zz}}{\partial z} + \rho f_z \tag{4}$$

$$\frac{\partial}{\partial t}(\rho E) + \nabla.(\vec{V}(\rho E + p)) = \nabla.(k_{eff}\nabla T - \sum_j h_j \vec{J_j} + (\overline{\overline{\tau_{eff}}}.\vec{V} \tag{5}$$

$$\frac{\partial}{\partial t}(\rho k) + \frac{\partial}{\partial x_i}(\rho k u_i) = \frac{\partial}{\partial x_j}\left[\left(\mu + \frac{\mu_t}{\sigma_k}\right).\frac{\partial k}{\partial x_j}\right] + G_k + G_b - \rho\varepsilon - Y_m + S_k \tag{6}$$

$$\frac{\partial}{\partial t}(\rho \varepsilon) + \frac{\partial}{\partial x_i}(\rho \varepsilon u_i) = \frac{\partial}{\partial x_j}\left[\left(\mu + \frac{\mu_t}{\sigma \varepsilon}\right).\frac{\partial \varepsilon}{\partial x_j}\right] + C_{1\varepsilon}.\frac{\varepsilon}{k}(G_k + C_{3\varepsilon} + G_b) - C_{2\varepsilon}.\rho.\frac{\varepsilon^2}{k} + S_\varepsilon \tag{7}$$

Convection and radiation heat transfer have a significant impact on the indoor fluid flow. Indoor comfort and energy demand research require a comprehensive analysis of radiation and convection heat transfer because small changes can have a significant impact on indoor comfort. Electromagnetic waves are the form in which heat radiation transfer occurs, and the following DO radiative transport model can be used to predict it [32][33]:

$$\nabla(I(\vec{r},\vec{s})\vec{s}) + (a+\sigma_s)I(\vec{r},\vec{s}) = an^2\frac{\sigma T^4}{\pi} + \frac{\sigma_s}{4\pi}\int_0^{4\pi} I(\vec{r},\vec{s}')\times\phi(\vec{r},\vec{s}')d\Omega' \quad (8)$$

The total heat load of the radiator is calculated using Equation 9,

$$Q_{total\ heat\ load} = Q_{convection} + Q_{radiation} \quad (9)$$

The temperature of the indoor air will change depending on the ventilation settings. The usual range of 3 to 5 W/m^2-K for gases is the convective heat transfer coefficient for convection. The heat transfer by convection and radiation between the radiator surface and the inside air is represented by the following equation (Equations 10, 11) [34][35].

$$Q_{Conv} = A_{rad\ Surf} \times h_{Conv} \times (T_{rad} - T_{amb}) \quad (10)$$

$$Q_{Radiation} = \sigma \times \varepsilon_{black} \times A_{rad\ Surf} \times ({T_{rad}}^4 - {T_{amb}}^4 \quad (11)$$

Once the numerical simulation is fully converged, the PMV and PPD indices are evaluated in a steady-state environment formulated by Fanger and Toftum [36] as shown in Equations 12-16. The stability and dependability of the results, validated by this method, guarantee an equilibrium state with constant IEQ inside the simulated environment.

$$\begin{aligned} PMV = (3.03e^{-0.036M} + 0.028(M-W) - 3.05 \times 10^{-3}[5733 - 6.99(M-W) - p_a] \\ - 0.42[(M-W) - 58.15] - 1.7 \times 10^{-5}M(5867 - p_a) - 0.0014M(34 - T_{av}) \\ - 3.96 \times 10^{-8} f_{cl}[(T_{cl}+273)^4 - (\bar{T}_r + 273)^4] - f_{cl}h_c\,(T_{cl} - T_{av}) \end{aligned} \quad (12)$$

$$T_{cl} = 35.7 - 0.028\,(M-W) - I_{cl}\{3.96 \times 10^{-8} f_{cl}\,[(T_{cl}+273)^4 - (\bar{T}_r + 273)^4] + f_{cl}h_c\,(T_{cl} - T_a)\} \quad (13)$$

$$h_c = \begin{cases} 2.38\,(T_{cl} - T_{av})^{0.25} & 2.38\,(T_{cl} - T_{av})^{0.25} > 12.1\sqrt{U} \\ 12.1\sqrt{U} & 2.38\,(T_{cl} - T_{av})^{0.25} < 12.1\sqrt{U} \end{cases} \quad (14)$$

$$f_{cl} = \begin{cases} 1.00 + 1.290I_{cl} & I_{cl} > 0.078\dfrac{m^2K}{W} \\ 1.05 + 0.645I_{cl} & I_{cl} < 0.078\,m^2K/W \end{cases} \quad (15)$$

$$PPD = 100 - 95 \times e^{(-0.03353\,PMV^4 - 0.2179\,PMV^2)} \quad (16)$$

The inlet air velocity was maintained below 0.7 m/s to minimise indoor turbulence, eddies, and cold drafts for the occupants. Low inlet velocity results in a low Reynolds number (Ringlet > 600), indicating incompressible flow with natural convection ($\frac{Gr}{Re^2} \ll 1$). The subsequent dimensionless numbers in equations 17-19 give the further calculations,

$$Re = \frac{\rho VL}{\mu} \quad (17)$$

$$Gr = \frac{g\beta(T_{radiator} - T)L^3}{\upsilon^2} \quad (18)$$

$$Ra = \frac{g\beta(T_{radiator} - T)L^3}{\upsilon\alpha} \quad (19)$$

As mentioned above, natural convection fluids follow the Boussinesq approximation and can be solved using RANS equations by adding the parameter to the momentum equation.

2.4 Comfort Parameters

This study uses various techniques to evaluate indoor occupant comfort. The operating temperature is similar to the steady-state temperature in a hypothetical black room, where heat exchange from radiation and convection occurs at the same rate as in a real, non-uniform environment. It is determined by averaging indoor air temperature and radiation, which together affect indoor comfort metrics. Surfaces that radiate heat cause variations in the operative temperature within the fluid domain. The closer surfaces produce higher operating temperatures, which are also affected by emission power and view factor. Comfort temperature, on the other hand, takes into account both the air velocity inside the building and the air temperature. It considers how air velocity affects thermal comfort, especially in cold climates where air velocity close to occupants is > 0.1 m/s, which creates discomfort. The temperature gradient between the ankle and neck level is another parameter used in comfort assessment. ISO7730 recommends that the gradient should not exceed 1.5ºC to prevent discomfort for occupants.

The equations for operating temperature and comfort temperature are as follows:

$$T_{operative} = \frac{T_{air\ temperature} + T_{Radiation\ temperature}}{2} \quad (20)$$

$$T_{Radiation}{}^4 = \frac{1}{4.\sigma}\int_0^{4\pi} Id\Omega \tag{21}$$

$$T_{Comfort} = \frac{T_{Radiation} + T_{Air}\sqrt{(10.v_{Air})}}{1+\sqrt{(10.v_{Air})}} \tag{22}$$

$$V_{air} - Air\ velocity\ \left(V_{air} \geq 0.1\frac{m}{s}\right)$$

$$T_{Air} - Air\ Temperature$$

2.5 Numerical and Experimental Validation

Comfort temperature was numerically validated and compared to an experimental study by Olesen *et al.* [30] to ensure model accuracy. An empty room, replicating the experimental setup in terms of boundary conditions, was employed for validation. Figure 3 illustrates similar trends in both the experimental and numerical comfort temperature profiles. Furthermore, numerical results were compared to the work of Horikiri *et al* [31] for additional validation. Comfort temperatures at four specific monitoring locations within the empty room model were compared between this study and the above-mentioned numerical and experimental analysis. The model accuracy was established through comparisons with established experimental [30] and numerical data [31], exhibiting a maximum deviation of ±0.5°C.

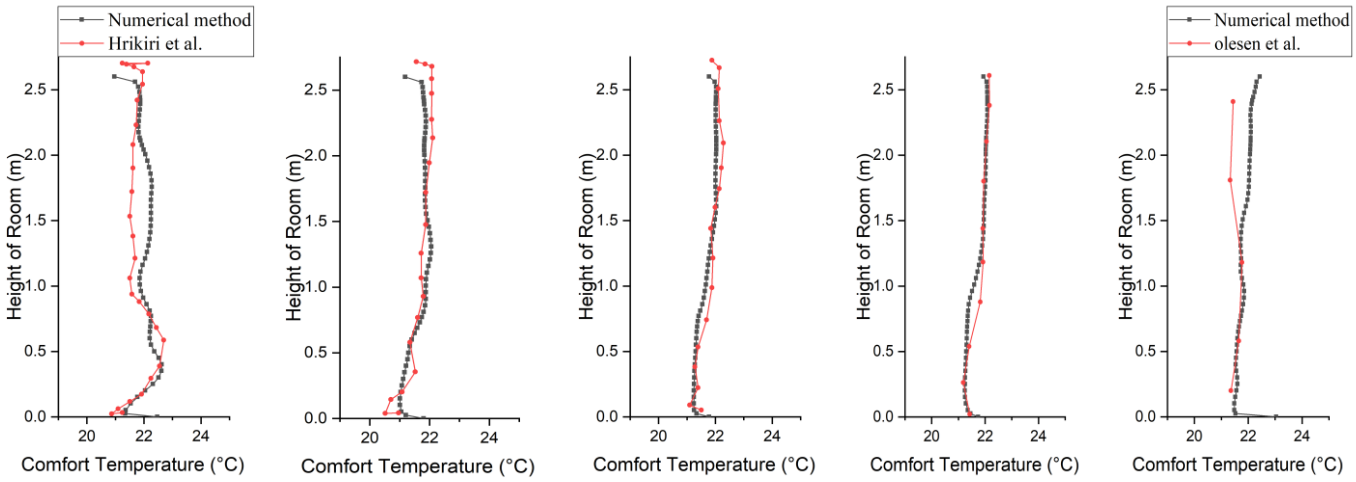

Figure 3. Validation of CFD model with Horikiri *et al.* (Z = 0) [29] (a) h_1=0.6m, (b) h_2=1.8m, (c) h_3=3.0m, (d) h_4 = 4.2m, and experimental results by Olesen *et al.*[30] at (e) h=1m

This study is supported by the established validation processes from a previous study [32], which validated the precision of the numerical model for steady-state fluid flow.

3. RESULT AND DISCUSSION

A further numerical study followed the validation of the 3-D geometric model with peer-reviewed experimental and numerical work. Following the acceptable validation results, the geometry was modified to conduct the present study. Additional analyses of IEQ and occupant comfort examined various occupant comfort parameters across different case studies.

3.1 Indoor Air Temperature

As discussed in an earlier section, air temperature is a significant factor that marks the comfort of indoor occupants and overall IEQ. This section studies comfort based on operative temperature trends, total temperature contours, and temperature gradients. Figure 4 shows the comfort temperature trends for the different case studies. A significant discrepancy is present in the area adjacent to the radiator, due to the strong buoyancy force in all the cases. The radiator position alters the operative temperature. For cases 1 and 2, where the outlet vent is located on the same wall but at a distant location from the floor. The comparison shows no considerable variation in the operative trends. Similarly, the operative temperature in the region near the outlet vent also fluctuates for that particular location near the outlet vent. This discrepancy in the operative temperature is not present for the outlet vent at the top of the wall. For case 3, the lowest temperature is at the floor level, while the overall temperature distribution in the indoor fluid domain also shows an unstable fluid domain. The indoor air temperature should be stable and uniform for acceptable indoor thermal comfort [2]. The possible cause for the lower temperature in the floor region may be due to the less effective buoyancy effect, which is responsible for the intermixing of the hot and cold indoor air. The relatively lower temperature in the fluid domain results when all the outlet vents are active. The discrepancy in the indoor operative temperature is lower, but the overall fluid domain operative temperature reduces due to the less effective buoyancy phenomenon.

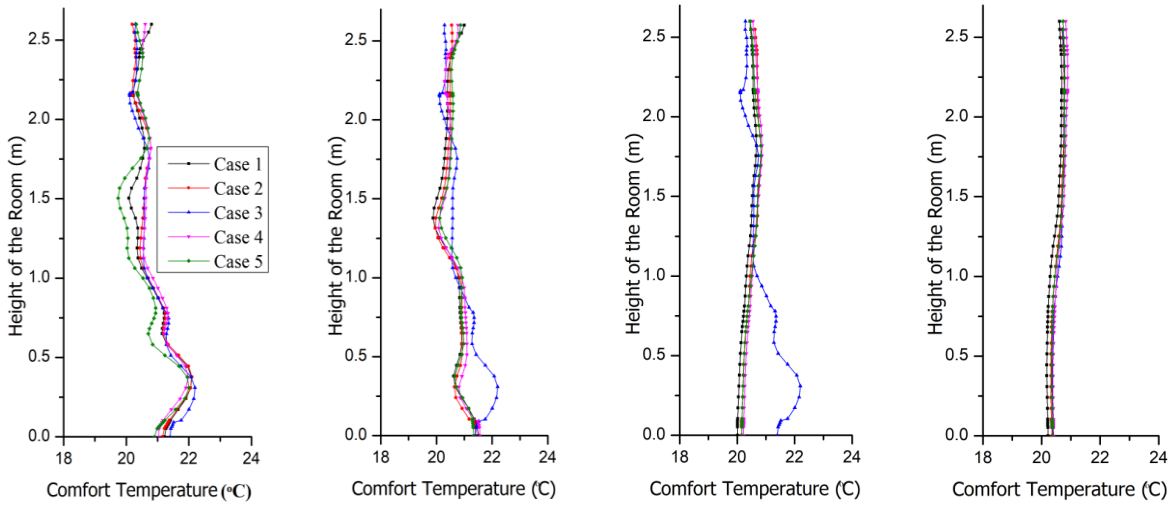

Figure 4. Operative temperature of the indoor fluid domain at four different locations (a) 0.6 m, (b) 1.2 m, (c) 3.0 m, and (d) 4.2 m from the radiator

Cases with floor-level outlet vents achieved a stable operative temperature. Hence, locating the outlet vent away from the occupancy is recommended when a stable temperature is required for occupant comfort [33]. Total temperature contours are plotted for a more effective analysis of IEQ and computed as a post-processing result on the mid-plane. Figure 5 (a)-(e) shows the uniform stratification layers on the contour, indicating the stable indoor air temperature. The region near the floor is at a lower temperature than the ceiling, as shown in the contours, due to the buoyancy phenomenon.

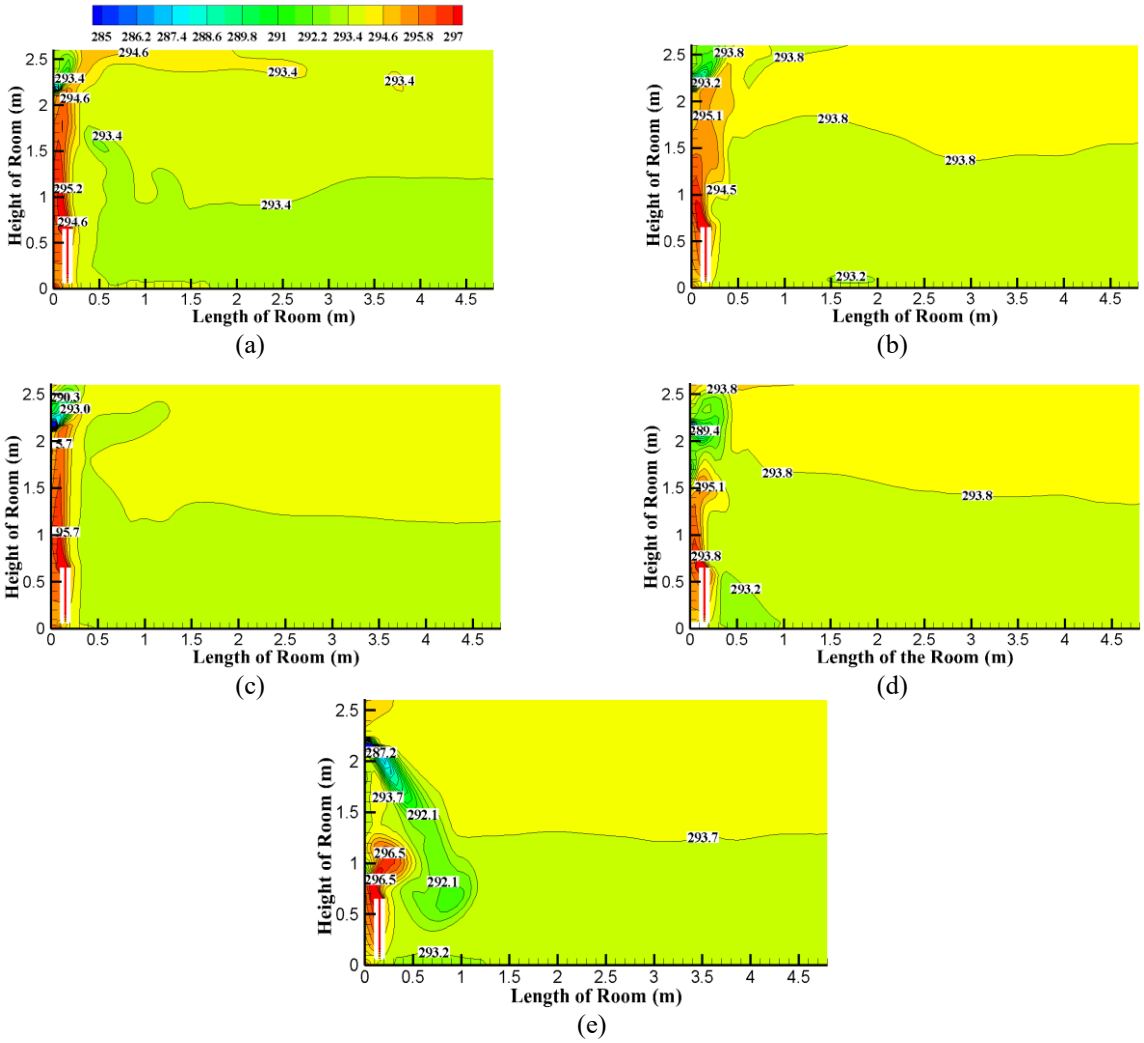

Figure 5. Total temperature contours for a plane passing through the room (Plane XY) (Z=0) (a) case 1, (b) case 2, (c) case 3, (d) case 4, (e) case 5

Although the operative temperature is lower for case 3, the total temperature is somewhat similar, with only minor variations across all cases. The mixing zone length varies across different configurations. Case 5, where all outlet vents are active, exhibits the highest mixing zone length. The larger mixing zone results in a reduced occupied zone where the indoor occupant can reside. High turbulence in the mixing zone prevents sustaining adequate comfort conditions in this region. For ideal conditions, the mixing zone should be minimal, and the occupied zone should be larger to accommodate a large number of occupants indoors with acceptable comfort conditions.

In case 3, with outlet vents symmetrical to the fluid domain and positioned closer to the floor, the mixing zone is smaller, resulting in a more uniform indoor air temperature. The next important factor that governs the comfort of the indoor occupant is the vertical temperature gradient. The temperature gradient for the different cases has been calculated using the temperature difference between the imaginary occupants sitting on the chair, which has a height of 1.3 m from the floor level, as shown in Figure 6.

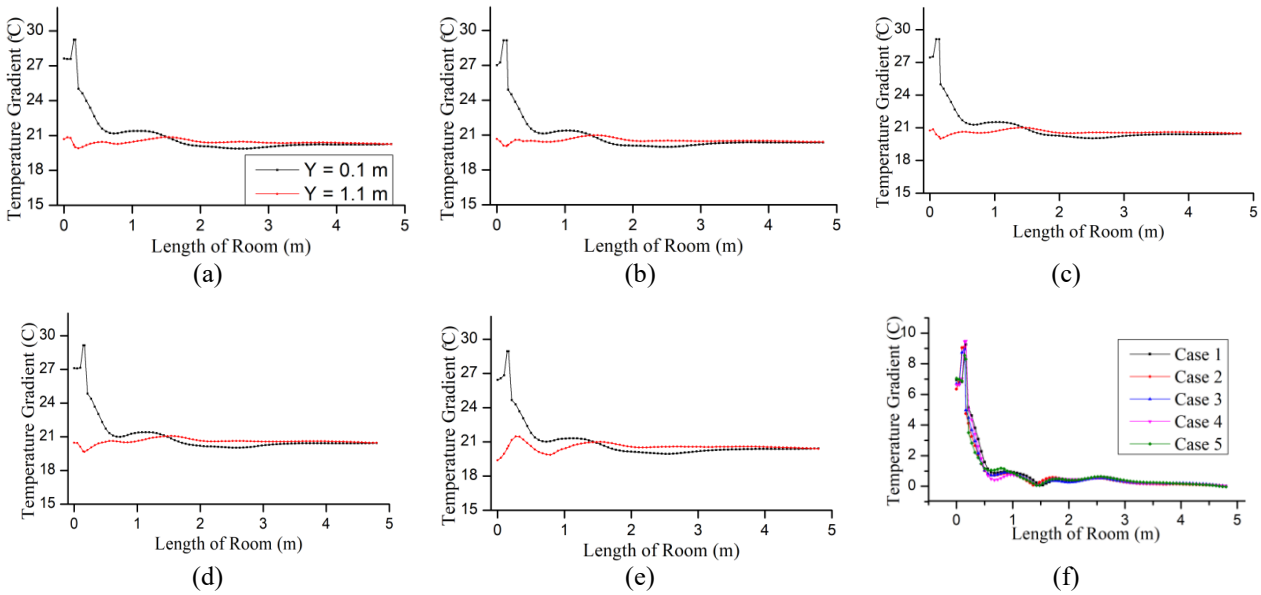

Figure 6. (a)-(e) Air temperature trends for different cases at height of Y=0.1 m, and Y = 1.1 m from the floor level, (f) Temperature gradient for the different cases

The study highlights several trade-offs in achieving optimal thermal comfort. Placing the outlet vent closer to the floor, as seen with outlet 1, increases turbulence and reduces the occupied zone, which negatively impacts comfort. In contrast, placing the outlet vent higher on the wall for cases with outlet 3 and outlet 4 active minimises turbulence but may reduce the effectiveness of air mixing in certain areas. Increasing the mixing zone when all outlets are active helps in reducing localised hot spots, but results in a smaller occupied zone, which leads to discomfort due to high turbulence. A smaller mixing zone, resulting from the placement of outlet 2 and outlet 4, creates better comfort conditions but may cause temperature variations near the floor due to weaker buoyancy effects. The trade-off between temperature uniformity and buoyancy effects is carefully managed, as higher buoyancy near the radiator may increase comfort but also create temperature divergences. Therefore, optimising outlet vent placement, mixing zones, and temperature distribution is crucial for balancing comfort and energy efficiency.

3.2 Air Velocity

The airspeed in the occupied area is the second most significant factor to consider when analysing indoor occupant comfort and overall IEQ. The calculated indoor air velocity, including the air velocity magnitude, is presented at four different monitoring lines for each case. Figure 7 illustrates that the area near the radiator and inlet vent exhibits a strong buoyancy effect, resulting in higher air velocities in that region. The air velocity magnitude in other areas, away from the radiator, is lower than 0.1 m/s, which is suitable for occupant comfort and maintains an acceptable level of indoor comfort. Each monitoring line shows an increase in velocity magnitude around the exhaust vent. The velocity is higher in the region close to the ceiling compared to the other fluid domains.

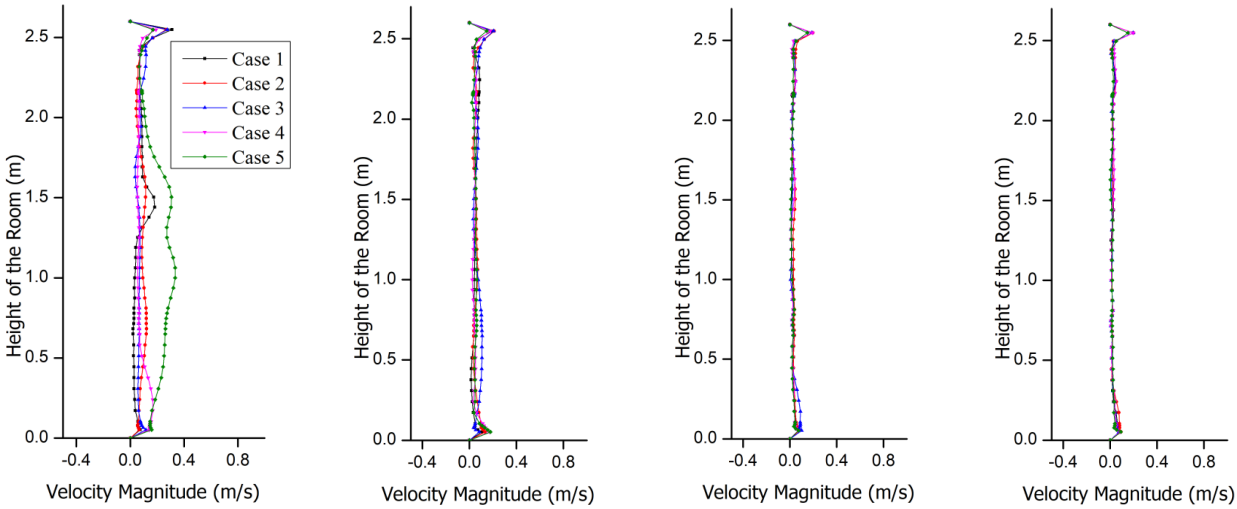

Figure 7. Velocity magnitude of the indoor fluid domain at four different locations (a) 0.6 m, (b) 1.2 m, (c) 3.0 m, and (d) 4.2 m from the radiator

The velocity magnitude decreases and becomes constant for all ventilation setups, except near the radiator. The results indicate that outlet ventilation conditions have a minimal impact on the air velocity inside the building, allowing designers to disregard this effect during ventilation system planning. The outlet vent location influence on the velocity magnitude is not considerable in the X direction, as discussed above. The effect of different outlet vent locations on the velocity magnitude in the Y direction can be analysed using the horizontal monitoring lines. Figure 8 illustrates the air velocity magnitude trends at P_1, P_2, P_3, and P_4. The velocity magnitude in the area close to the radiator is notably high, making this region unsuitable for occupancy.

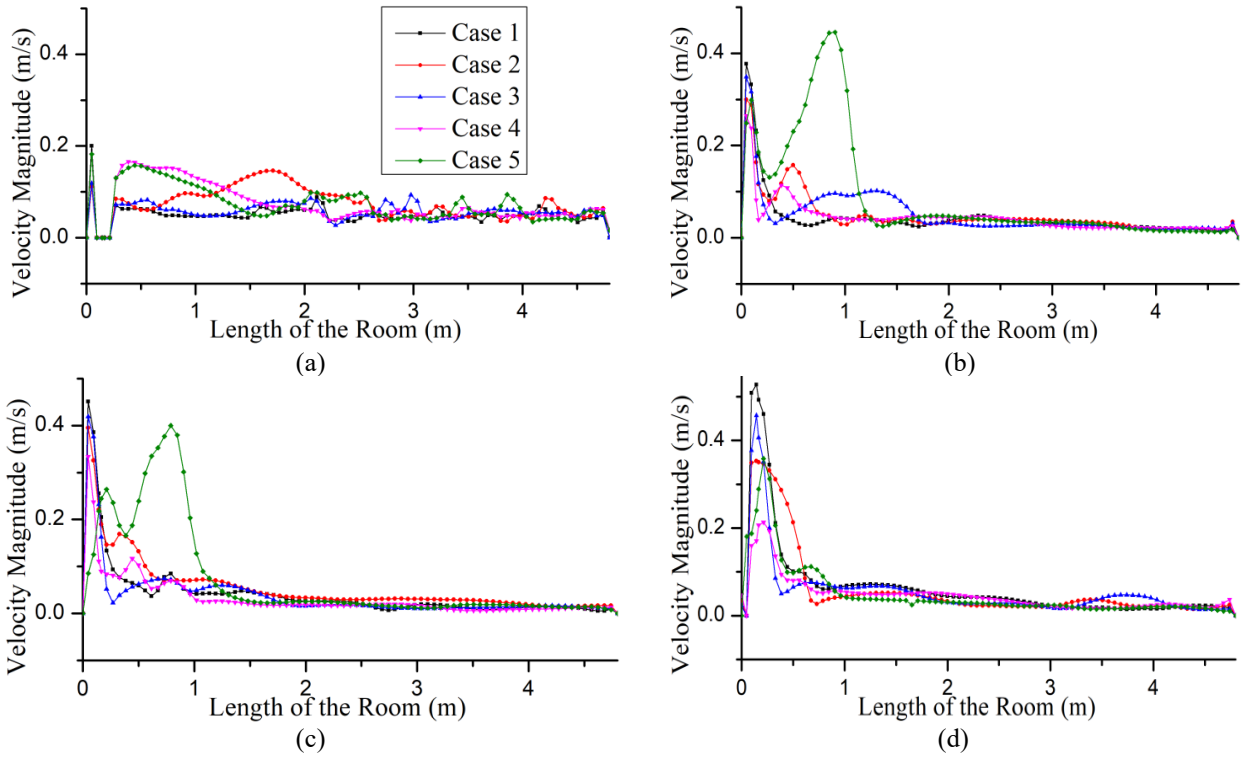

Figure 8. Velocity magnitude of the indoor fluid domain at four different locations (a) 0.1 m, (b) 0.8 m, (c) 1.1 m, and (d) 2.0 m from the radiator

For case 5, when all the outlet vents are active, the magnitude of the air velocity is considerably higher, especially near the radiator. This region of the higher velocity accounts for the discomfort to the occupant. The velocity magnitude in the region near the floor at Y= 0.1 m is higher and exceeds the limiting value of the air velocity magnitude for indoor occupant comfort. The velocity magnitude in the other regions is identical in magnitude and steady for all ventilation configurations. It indicates that the velocity magnitude in regions other than the floor region and mixing zone is independent of the type of outlet ventilation configuration used for different cases. As the distance from the radiator increases, the mixing length reduces, and the occupied zone increases.

Velocity vector contours for the other cases illustrate the indoor air velocity across different case studies, as shown in Figure 9. The contours of the velocity vectors help find eddies and circulations indoors. Higher eddies and circulation occur when the outlet vent is located at the floor level compared to the ceiling level. Case 5, with all outlet vents active, exhibited the highest average velocity magnitude. Case 3, featuring outlet vents near the floor level on both sides of the symmetric model, exhibited high-intensity circulations. The observations from the velocity vector contours indicate that the outlet vents located at the floor level of the building may introduce more indoor fluid turbulence.

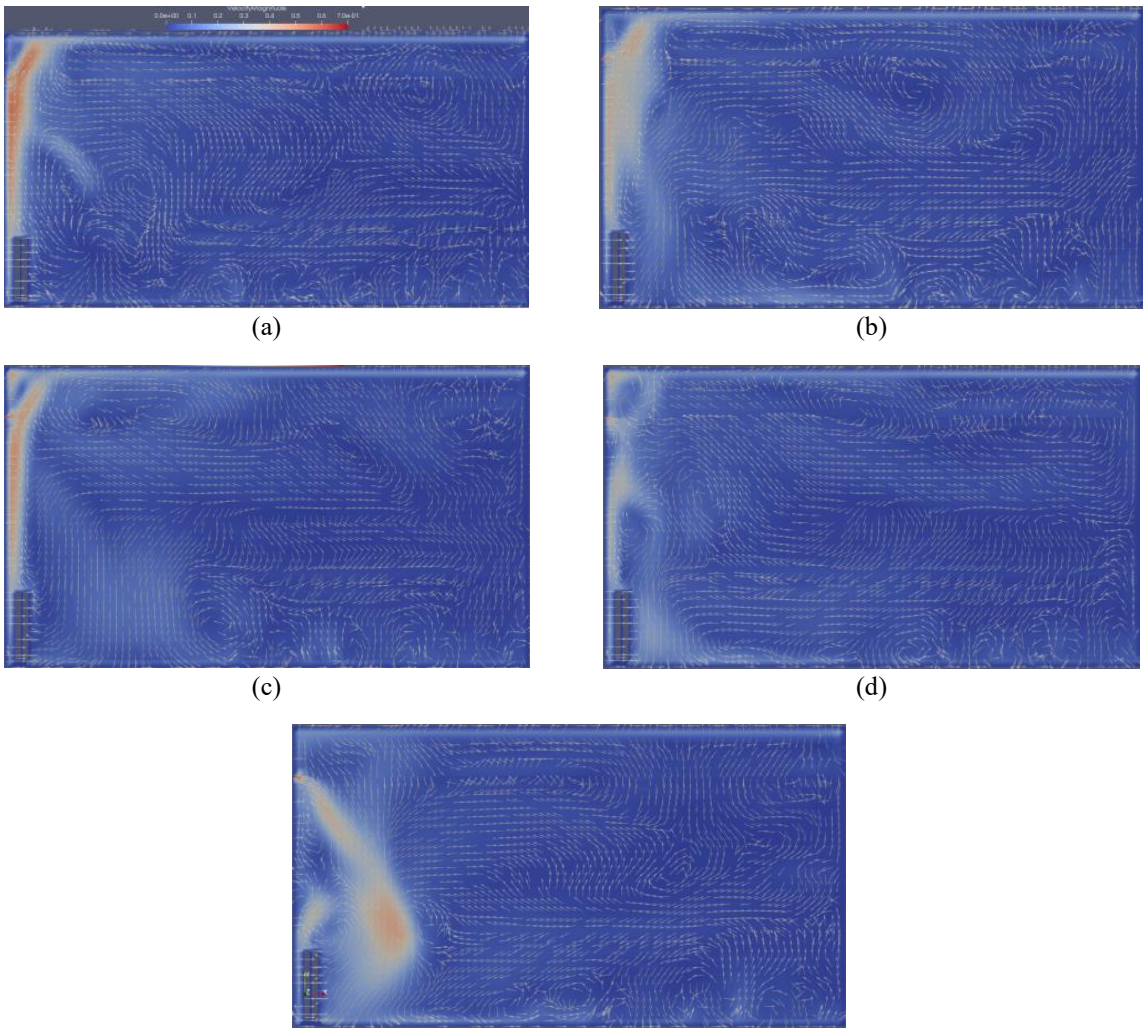

(a) (b) (c) (d) (e)

Figure 9. Velocity vector of the indoor fluid domain on a plane passing through the centre of the fluid domain (z = 0) for (a) case 1, (b) case 2, (c) case 3, (d) case 4, (e) case 5

Although eddies and circulations are considerable in all cases, the velocity vectors change with the changing outflow location. It indicates that the position of the outlet ventilation configuration affects the velocity vector and flow patterns in the fluid domain. The results are then further interpreted to highlight key implications and trade-offs. The outlet vent positions closer to the floor increase turbulence and reduce comfort, and a higher location improves stability but may reduce air mixing efficiency. Activating all outlets enhances mixing but reduces the comfort occupied zone due to increased velocity and air circulation. These insights help to balance thermal comfort with ventilation effectiveness in designing the building envelope.

3.3 Comfort Evaluation of Indoor Occupants

A hypothetical occupant wearing winter clothing with 0.1 clo clothing insulation was studied to assess the comfort level of an indoor occupant. The occupant is considered a non-voluntary heat-generating surface, and low activity levels were selected. The PMV and PPD models are used to calculate the comfort of potential indoor occupants performing low-activity tasks, such as sitting in a chair, reading, or writing. Fanger et al. [36] utilised occupant comfort data and the characteristics of the indoor environment to develop PMV and PPD models for analysing multiobjective indoor occupant comfort. The PMV and PPD models are now the most widely used. These guidelines take into account various factors, including air velocity, clothing insulation, metabolic rate, and operating temperature. Some researchers have criticised these models for their uniform comfort assumptions despite their widespread use and abundant documentation [34]. However, most indoor comfort evaluations favour this model [35]. The models estimate occupant comfort under thermally stable conditions, from hot to cold, and cover a specific temperature range of 10 to 35°C. These models, which are widely

accepted by the ISO 7730 and ASHRAE 55 standards, are essential for generating valuable data on indoor comfort [36]. The PMV model developed by Fenger et al. takes into account all relevant comfort analysis elements based on heat balance [37][38]. The heat load and comfort index constraints with normalised values for different cases are mentioned in Tables 3 and 4, respectively.

Table 3. Comfort constraints

Case study	Heat load (L)	PMV Index	PPD Index
1	418.84	0.27	7.08
2	412.27	0.24	7.12
3	412.70	0.21	8.76
4	413.52	0.32	8.27
5	413.26	0.51	12.11

Table 4. Normalised values of the comfort constraints

Case Study	$(L_i)_{Normalized}$	$(PMV_i)_{Normalized}$	$(PPD_i)_{Normalized}$
1	1.00	0.20	0.00
2	0.00	0.10	0.00795
3	0.065	0.00	0.3348
4	0.190	0.37	0.2364
5	0.151	1.00	1.00

The key comfort trade-offs were analysed using PMV and PPD data to enhance the interpretation of the results. Case 2 shows the best performance with the lowest heat load (412.27 W) and minimal discomfort (PPD = 7.12), which makes it the most energy-efficient and comfortable setup. Case 1 has the highest heat load (418.84 W) but maintains low discomfort (PPD = 7.08), indicating a comfort-energy trade-off. Case 3 presents a good compromise with the lowest normalised PMV, though its PPD is slightly higher (8.76). In contrast, Case 5, with all outlets active, results in the highest discomfort (PPD = 12.11) and does not offer significant energy benefits. It shows that excessive ventilation can reduce comfort without improving efficiency. These findings suggest that careful outlet placement optimises both comfort and energy use, while excessive ventilation should be avoided to prevent discomfort.

3.4 Energy Demand

The design of sustainable buildings demands the proper balance between building energy consumption and indoor occupant comfort. The optimal balance can be achieved by analysing the energy requirements of the building under various outlet ventilation conditions and selecting the model with the lowest energy consumption. The various parameters affecting the energy consumption by the radiator have been computed and tabulated in Table 5.

Table 5. Heat load on the radiator

case	h ($W/m^2 \cdot K$)	$T_{Radiator}$ (K)	T_{amb} (K)	$Q_{Convection}$ (W/m^2)	$Q_{Radiation}$ (W/m^2)	Q_{Total} (W/m^2)	Percent increase
1	2.42	309 K	293.55	117.77	301.07	418.84	1.60
2	2.36	309 K	293.69	113.78	298.49	412.27	0.00
3	2.39	309 K	293.72	114.74	297.96	412.70	0.10
4	2.43	309 K	293.76	116.35	297.16	413.52	0.30
5	2.41	309 K	293.73	115.57	297.69	413.26	0.23

Case 2 exhibits the lowest heat transfer coefficient, while case 4 shows the lowest radiator radiation load for maintaining indoor thermal comfort. The exhaust vent at the base of the wall has the lowest total heating load on the radiator. A case 2 study has been used as a baseline for comparison because it has the lowest heating load on the radiator. When the output vent is close to the ceiling, the ventilation setting will show the highest heating load. The dominant buoyancy effect in the indoor setting may cause this behaviour. Buoyancy effects cause warm air to rise to the ceiling, and if the outlet vent is close to the ceiling, warm air can escape from the indoor environment by reducing the average temperature of the indoor air. Increasing the radiator heating load compensates for the drop in indoor air temperature to maintain indoor comfort. The outlet vent near the floor traps warm air near the ceiling while cold indoor air settles on the floor, allowing it to escape from the indoor environment. It reduces the heating load on the radiator to maintain indoor thermal comfort by allowing cold air to escape into the indoor environment while trapping warm air near the ceiling. Hence, the average heat energy added by the radiator to the indoor air is minimal in this case. Radiation heat transfer is unaffected by the convection heat transfer coefficient, while a low natural heat transfer coefficient reduces convection heat transfer from the radiator. Poor mixing of hot and cold air due to low turbulence around the radiator causes low fluid

flow with reduced eddies and circulation in this region, resulting in a low convection heat transfer coefficient and a low Reynolds number. This effect can be integrated for a large building with a high occupancy rate, even though the fluctuations in the total heat load on the radiator for different conditions show minimal variation. Although the total heat load on the radiator changes slightly (within 1.6%), the vent placement affects how efficiently the radiator maintains comfort.

The setup with the outlet near the floor (412.27 W) uses the least energy. It helps to trap warm air inside and let cold air exit, which reduces the radiator load. In contrast, when the outlet is near the ceiling (418.84 W), warm air escapes, which lowers the room temperature and increases the heating load on the radiator. Lower convection heat transfer (2.36 W/m²·K) shows less air mixing and heat loss, but it may also lead to uneven temperatures. These findings show that proper outlet placement is key to saving energy and keeping indoor comfort balanced.

3.5 Optimisation of the IEQ

The problem of indoor comfort involves various aspects that determine the optimal solution for a building, considering the occupant's comfort while minimising energy consumption. Establishing a suitable balance between occupant well-being and building energy demand ensures the required comfort for optimum IEQ. Multiobjective Optimisation (MOO) techniques can optimise both energy use and indoor comfort. The most common method in the optimisation of the MOO is the Weighted Sum Method (WSM). It is a popular and straightforward technique used in MOO to combine multiple conflicting objectives as a single objective. It involves assigning weights to each aim to reflect their relative importance, and then optimising the combined objective function. Table 6 shows the calculated normalised values of the comfort parameters and radiator heat load. The problem is of minimising the objective function, as it requires a balancing trade-off between the different parameters. The lowest energy consumption is obtained for case 2, while the lowest PMV and PPD indices are observed for cases 3 and 1, respectively. The acceptable constraints observed for the different cases apply to the defined objective function. This function should balance all the factors to optimise the relationship between indoor energy consumption and indoor occupant comfort.

The first objective is to minimise the energy consumption of the building required for maintaining indoor comfort, and the second objective is to improve occupant comfort, which includes the minimum PMV and PPD index. A 50% weightage has been allocated to both objectives to maintain a proper balance between energy demand and occupant comfort. This study calculated the normalised values for the other objective parameters using the optimisation equations to develop the objective functions for the different case studies. The team then used these normalised values to determine the objective function for each case study. Equations 23-26 show the equations for the normalised values of the various constraints needed to optimise the IEQ.

$$(L_i)_{Normalized} = \frac{L_i - L_{min}}{L_{max} - L_{min}} \tag{23}$$

$$(PMV_i)_{Normalized} = \frac{PMV_i - PMV_{min}}{PMV_{max} - PMV_{min}} \tag{24}$$

$$(PPD_i)_{Normalized} = \frac{PPD_i - PPD_{min}}{PPD_{max} - PPD_{min}} \tag{25}$$

$$F(x)_i = W_L.L_i + W_{PMV}.PMV_i + W_{PPD}.PPD_i \tag{26}$$

Table 6. Optimised objective functions

case study	Objective function $(F(x)_i)$	Function value
1	$F(x)_1 = 0.5 \times 1 + 0.25 \times 0.20 + 0.25 \times 0$	0.550
2	$F(x)_2 = 0.5 \times 0 + 0.25 \times 0.10 + 0.25 \times 0.0079$	0.026
3	$F(x)_3 = 0.5 \times .065 + 0.25 \times 0 + 0.25 \times 0.334$	0.116
4	$F(x)_4 = 0.5 \times 0.19 + 0.25 \times 0.37 + 0.25 \times 0.236$	0.246
5	$F(x)_5 = 0.5 \times 0.15 + 0.25 \times 1 + 0.25 \times 1$	0.575

Table 6 shows the functions for different cases that need to be optimised and the calculated function values. The minimum value of the function shows a better trade-off between the conflicting objectives as discussed in the previous section. The objective function for case 2 shows the minimum value, which indicates the proper balancing between the building energy demand and the acceptable comfort parameters. The analysis shows that the ventilation strategy used in case 2, with the outlet vent located near the floor and cross ventilation applied, provides the optimum solution for the present problem. The analysis determined the next optimised function value for case 3, where the outlet vents are located at the floor level. The maximum function value occurs in cases 5 and 1, with case 5 having all vents open. This may be due to the weak comfort conditions for the occupant in this type of ventilation setting, resulting from the increased air velocity magnitude discussed in section *3.2 Air Velocity*. The analysis identifies the best compromise solution for the

ventilation setting with outlet vents located at the floor level. Specific configurations perform better due to how they manage airflow and heat retention. Outlet vents near the floor help to trap warm air in the occupied zone and let cold air exit, which reduces the radiator heat load (as low as 412.27 W) while maintaining comfort.

In contrast, ceiling-level outlets allow warm air to escape due to buoyancy, increasing the heat load (up to 418.84 W) and reducing energy efficiency. Thus, outlet placement directly impacts both comfort and energy use. The lower outlets offer better balance, while outlets near the ceiling may improve airflow but require more heating. This study shows that outlet vent location affects IEQ based on its height and distance from heat sources and inlet vents. In symmetric fluid domains, symmetric outlet placement improves energy efficiency and occupant comfort. Outlet position does not significantly affect temperature gradients or air velocity in cold climates, but floor-level vents can create more eddies in the occupied zone. The effect on energy demand is minor; it may increase in high-volume spaces and with increased occupancy. Optimising vent placement helps balance radiator heat load and comfort, supporting sustainable building design.

4. CONCLUSIONS

This research investigates the influence of altered ventilation configurations on the IEQ and building energy demand, depending on the location of the outlet vents. Using ANSYS Fluent software, a 3-dimensional fully validated geometric model is created and validated with numerical and experimental data. The previous discussion shows that different outlet ventilation locations suit the specific necessities of the building model. The following lists the significant findings:

- For buildings with symmetric fluid domains, employing symmetrical outlet vent placement significantly improves thermal comfort and energy efficiency. Case 2 demonstrated this clearly, achieving the lowest objective function value (0.026), with a heat load of 412.27 W, a PMV of 0.24, and a PPD of 7.12, providing a practical reference for real-world ventilation design.
- The study confirms that outlet vent position has a minimal effect on indoor temperature gradients in cold-climate conditions, making it a secondary factor when optimising for temperature uniformity.
- The analysis shows that outlet vent location negligibly impacts indoor air velocity across all cases, allowing designers to deprioritise air velocity in early-stage decisions for similar room layouts and conditions.
- Floor-level outlet vents, while often used in practice, can increase indoor air turbulence and reduce comfort. Case 5 recorded the highest PMV (0.51) and PPD (12.11), along with the highest objective function value (0.575), making it the least favourable configuration.
- Although the energy demand variation due to outlet location is relatively small, it becomes increasingly significant in larger indoor volumes and higher occupancy scenarios, where airflow complexity and heat load interactions intensify.
- A key practical contribution of this study is the implementation of a multi-criteria optimisation method using normalised PMV, PPD, and heat load values to evaluate ventilation performance. This method enables designers to balance thermal comfort and energy efficiency, making it applicable to sustainable HVAC planning in office buildings and similar indoor environments.

Careful selection of the outlet vent location, considering the existing indoor volume and layout, ensures a sustainable building with an appropriate indoor comfort index and a low radiator heat load. For larger fluid domains and occupancies, comparable outcomes can be integrated by scaling and integrating the appropriate perimeter.

ACKNOWLEDGEMENTS

This study was not supported by any grants from funding bodies in the public, private, or not-for-profit sectors.

CONFLICT OF INTEREST

The authors declare no conflicts of interest

AUTHORS CONTRIBUTION

G.A.Ganesh (Methodology; Data curation; Writing - original draft; Visualisation)

S.L.Sinha (Conceptualization; Formal analysis; Resources; Project administration; Supervision)

V. Panchore (Data curation; Software; Formal analysis)

T.N. Verma (Conceptualization; Formal analysis; Resources; Project administration; Supervision)

REFERENCES

[1] A. Hamburg, Ü. Palmiste, A. Mikola, and T. Kalamees, "Ventilation Strategies for Deep Energy Renovations of High-Rise Apartment Buildings: Energy efficiency and implementation challenges," *Energies*, vol. 18, no. 11, p. 2785, 2025.

[2] ASHRAE, 10P Guideline: Interactions Affecting the Achievement of Acceptable Indoor Environments, 2nd Public Review, Atlanta, USA: ASHRAE, 2010.

[3] X. Su, Y. Yuan, Z. Wang, W. Liu, L. Lan, and Z. Lian, "Human thermal comfort in non-uniform thermal environments: A review," *Energy and Built Environment*, vol. 5, no. 6, pp. 853–862, 2023.

[4] G. A. Ganesh, S. L. Sinha, T. N. Verma, and S. K. Dewangan, "Investigation of indoor environment quality and factors affecting human comfort: A critical review," Building and Environment, vol. 204, p. 108146, 2021.

[5] D. Kajjoba, R. Wesonga, J. D. Lwanyaga, "Assessment of thermal comfort and its potential for energy efficiency in low-income tropical buildings: a review," *Sustainable Energy Research*, vol. 12, p. 25, 2025.

[6] J. Wang, T. Zhang, S. Wang, and F. Battaglia, "Numerical investigation of single-sided natural ventilation driven by buoyancy and wind through variable window configurations," *Energy and Buildings*, vol. 168, pp. 147–164, 2018.

[7] V. Tuninetti, B. Ales, and T. Mora Chandía, "Numerical and experimental analysis of thermal stratification in locally heated residential spaces," *Buildings*, vol. 15, no. 14, p. 2417, 2024.

[8] Y. Cheng, J. Niu, Z. Du, and Y. Lei, "Investigation on the thermal comfort and energy efficiency of stratified air distribution systems," *Energy for Sustainable Development*, vol. 28, pp. 1–9, 2015.

[9] S. Zhang, J. Jiang, Y. Cheng, C. Huan, and Z. Lin, "Equivalent room air temperature-based cooling load estimation method for stratum ventilation," in Stratum Ventilation—Advanced Air Distribution for Low-Carbon and Healthy Buildings, S. Zhang, Y. Cheng, and Z. Lin, Eds. Singapore: Springer, 2024.

[10] G. A. Ganesh, S. L. Sinha, and T. N. Verma, "Effect of inlet airflow direction on the indoor environment of a naturally ventilated room using CFD," *International Journal of Engineering and Advanced Technology*, vol. 9, no. 3, pp. 580–591, 2020.

[11] A. Longhitano, V. Costanzo, G. Evola, and F. Nocera, "Microclimate investigation in a conference room with thermal stratification: An investigation of different air conditioning systems," *Energies*, vol. 17, no. 5, p. 1188, 2023.

[12] G. A. Ganesh, S. L. Sinha, T. N. Verma, and S. K. Dewangan, "Numerical simulation for energy consumption and thermal comfort in a naturally ventilated indoor environment under different orientations of inlet diffuser," *Building and Environment*, vol. 217, p. 109071, 2022.

[13] A. A. Sedighi, F. Haghighat, and F. Nasiri, "Strategic ventilation design for reducing airborne infection transmission in a two-story building: A numerical approach," *Building and Environment*, vol. 262, p. 111785, 2024.

[14] C. Zhang, Y. Bai, Z. Cao, et al., "Critical factors to formatting and stabilising the vortex flow in the vortex ventilation system," *Building Simulation*, vol. 18, pp. 403–421, 2025.

[15] S. Wu, L. Wu, and L. Xiao, "Effects of aspect ratio and inlet wind velocity on thermal characteristics of Trombe wall channel under different ventilation strategies: An indoor experiment," *Experimental Thermal and Fluid Science*, vol. 141, p. 110800, 2023.

[16] D. Qiao, S. Wu, N. Zhang, and C. Qin, "Optimising the return vent height for improved performance in stratified air distribution systems," *Buildings*, vol. 14, no. 4, p. 1008, 2024.

[17] P. O. Fanger, "Assessment of man's thermal comfort in practice," *Occupational and Environmental Medicine*, vol. 30, no. 4, pp. 313–324, 1973.

[18] P. V. Nielsen, "Analysis and design of room air distribution systems," *HVAC&R Research*, vol. 13, no. 6, pp. 987–997, 2007.

[19] Y. Balali, A. Chong, A. Busch, and S. O'Keefe, "Energy modelling and control of building heating and cooling systems with data-driven and hybrid models—A review," *Renewable and Sustainable Energy Reviews*, vol. 183, p. 113496, 2023.

[20] D. W. Etheridge and M. Sandberg, *Building ventilation: theory and measurement*, vol. 50. Chichester, UK: John Wiley & Sons, 1996.

[21] Y. Li, L. Li, X. Cui, and P. Shen, "Coupled building simulation and CFD for real-time window and HVAC control in sports space," *Journal of Building Engineering*, vol. 97, p. 110731, 2024.

[22] J. A. Myhren and S. Holmberg, "Flow patterns and thermal comfort in a room with a panel, floor, and wall heating," *Energy and Buildings*, vol. 40, pp. 524–536, 2008.

[23] T. Long, Y. Li, W. Li, S. Liu, J. Lu, D. Zheng, K. Ye, Z. Qiao, and S. Huang, "Investigation on the cooling performance of a buoyancy driven earth-air heat exchanger system and the impact on indoor thermal environment," *Applied Thermal Engineering*, vol. 207, p. 118148, 2022.

[24] S. Mohammadreza, P. A. Mirzaei, and N. Mohammad, "Improvement of k-epsilon turbulence model for CFD simulation of atmospheric boundary layer around a high-rise building using stochastic optimisation and Monte Carlo sampling technique," *Journal of Wind Engineering and Industrial Aerodynamics*, vol. 171, pp. 366–379, 2017.

[25] Z. Zhai, Z. Zhang, W. Zhang, and Chen, "Evaluation of various turbulence models in predicting airflow and turbulence in enclosed environments by CFD: Part-1: summary of prevalent turbulence models," *HVAC&R Research*, vol. 13, no. 6, pp. 1–21, 2007.

[26] C. Buratti, D. Palladino, and E. Moretti, "Prediction of Indoor Conditions and Thermal Comfort Using CFD Simulations: A Case Study Based on Experimental Data," *Energy Procedia*, vol. 126, pp. 115–122, 2017.

[27] K. Ravindra, N. Agarwal, and S. Mor, "Assessment of thermal comfort parameters in various car models and mitigation strategies for extreme heat-health risks in the tropical climate," *Journal of Environmental Management*, vol. 267, p. 110655, 2020.

[28] H. Wang, H. Wang, F. Gao, P. Zhou, and Z. J. Zhai, "Literature review on pressure–velocity decoupling algorithms applied to built-environment CFD simulation," *Building and Environment*, vol. 143, pp. 671–678, 2018.

[29] L. Huang and Z. Zhai, "Critical review and quantitative evaluation of indoor thermal comfort indices and models incorporating solar radiation effects," *Energy and Buildings*, vol. 224, p. 110204, 2020.

[30] B. W. Olesen, E. Mortensen, J. Thorshauge, and B. Berg-Munch, "Thermal comfort in a room heated by a different method," *ASHRAE Transactions*, vol. 86, Tech. Paper no. 2556, 1980.

[31] K. Horikiri, Y. Yao, and J. Yao, "Numerical optimisation of thermal comfort improvement for an indoor environment with occupants and furniture," *Energy and Buildings*, vol. 88, pp. 303–315, 2015.

[32] G. A. Ganesh, S. L. Sinha, and T. N. Verma, "Numerical simulation for optimisation of the indoor environment of an occupied office building using double-panel and ventilation radiator," *Journal of Building Engineering*, vol. 29, p. 101139, 2020.

[33] P. Niemann and G. Schmitz, "Impacts of occupancy on energy demand and thermal comfort for a large-sized administration building," *Building and Environment*, vol. 182, p. 107027, 2020.

[34] T. Cheung, S. Schiavon, T. Parkinson, P. Li, and G. Brager, "Analysis of the accuracy on PMV–PPD model using the ASHRAE Global Thermal Comfort Database II," *Building and Environment*, vol. 153, pp. 205–217, 2019.

[35] D. Khovalyg, O. B. Kazanci, H. Halvorsen, I. Gundlach, W. P. Bahnfleth, J. Toftum, and B. W. Olesen, "A critical review of standards for indoor thermal environment and air quality," *Energy and Buildings*, vol. 225, p. 109819, 2020.

[36] P. O. Fanger and J. Toftum, "Extension of the PMV model to non-air-conditioned buildings in warm climates," *Energy and Buildings*, vol. 34, no. 6, pp. 533–536, 2002.

[37] E. W. Shaw, "Thermal comfort: Analysis and applications in environmental engineering, by P. O. Fanger," *Royal Society of Health Journal*, vol. 92, no. 3, p. 164, 1972.

[38] ISO 15265, Ergonomics of the thermal environment – Strategy of evaluation of the risk for the prevention of constraints or discomfort under thermal working conditions, Geneva: International Standardisation Organisation, 2004.